Synthesis and Characterization of High-Energy Nanoparticles

Liza Mercado, Perla M. Torres, Lewis M. Gomez, Nairmen Mina, Samuel P. Hernández, Richard Lareau†, R. Thomas Chamberlain†, and Miguel E. Castro-Rosario*

Chemical Imaging Center and Center for Chemical Sensor Development, The University of Puerto Rico at Mayagüez, Department of Chemistry, Mayagüez, Puerto Rico 00682

Received: November 10, 2003; In Final Form: May 20, 2004

Atomic force microscopy (AFM), scanning electron microscopy (SEM), white light imaging measurements, and Raman microscopy were employed for the characterization of hexahydro-1,3,5-trinitro-1,3,5-*s*-triazine (RDX) nanoparticles deposited on glass substrate surfaces. The RDX nanoparticles were prepared by exposure of glass substrate surfaces to an aerosol jet containing RDX. The spectroscopic signature of RDX particles and the two known forms of the material, β and α RDX, are compared. Raman measurements reveal that RDX nanoparticles and β deposits have similar spectroscopic signatures between 750 and 1000 cm^{-1}.

1. Introduction

Nanosized explosives and energetic materials are attractive to engineer nanosized holes and trenches and for cleaning pinholes and clogged ducts for fluid transport, and may find applications as propellants. In addition, explosive nanoparticles can be used as validation standards to challenge the detection limits of modern instruments built for trace explosive detection.[1] Numerous challenges exist in physical chemistry that require careful studies aimed at understanding the physical properties of nanosized explosives and energetic materials.

Hexahydro-1,3,5-trinitro-1,3,5-*s*-triazine, better known as RDX, is a powerful secondary explosive and propellant developed for medical purposes at the end of the 19th century.[2] The existence of two forms of this material in the solid state was documented by McCrone over 50 years ago.[3] These forms are known as β RDX and the well-studied α RDX phase. The structural and spectroscopic differences of these two forms of RDX have been the subject of numerous studies and are well documented in the literature.[4−10] Previous works in vibrational spectroscopy have focused on RDX deposits that are a few micrometers in size.[4,9−12] The properties and vibrational spectra of submicrometer RDX particles have received less attention. Such measurements can provide valuable information to studies aimed at trace explosive detection and the development of nanostructured energetic materials.[13]

2. Experimental Section

Dispersed RDX particles were prepared on glass substrates by exposure of the desired substrate surface to an aerosol jet containing 500 ppm RDX in acetonitrile solution. The substrate surface was exposed to the aerosol jet for less than 2 s and allowed to dry in air for about 5 min after each exposure. About three shots of the aerosol jet are required to accumulate enough dispersed particles that can be observed with the optical microscope. Experiments were performed in which hot nitrogen gas was used to evaporate the solvent from the jet during its flight to the target. In these experiments, a beam of hot nitrogen gas exited a 1/4 in. copper tube oriented perpendicular to the direction of flight of the RDX in acetonitrile jet.

Scanning electron microscopy (SEM), atomic force microscopy (AFM), and optical and Raman microscopy were employed for the characterization of the RDX nanoparticles. SEM measurements were performed with a Philips FEG-SEM XL30 system. The SEM has capabilities for energy-dispersive X-ray analysis (EDX). A gold coating (2.8 nm thick) was used to improve the electrical conductivity on the RDX deposits. Unless otherwise stated, a 2 kV accelerating voltage was employed for the SEM images. All SEM images were obtained in a vacuum chamber at a pressure of 3×10^{-5} mbar. AFM measurements were performed with a Nanonics 100 AFM system in the tapping mode and a 150 nm glass tip. White light images reported here were obtained with the RM 2000 Leica microscope. The microscope was validated with a commercial Olympus 0.1 mm micrometer ruler. Thus, the scales in the white light images reported here represent actual dimensions.

A Renishaw 2000 RM Raman microscope was employed for the acquisition of Raman spectra between 750 and 1000 cm^{-1}. The 785 nm line from a solid-state laser was used as the excitation source for the Raman measurements reported here. Previous works on UV−visible absorption measurements indicate that RDX absorbs between 193 and 330 nm.[14] Thus the Raman measurements reported here are nonresonant experiments. The Raman spectrometer was calibrated with CCl_4 and cyclohexane. The 785 nm laser light impinging on the samples has a rectangular shape with dimensions sensitive to the objective used in the microscope. A 1×3 μm rectangle is obtained when the laser light is focused on the sample through an objective with a magnification factor of 100×. A smaller rectangle, 0.5×1.5 μm, is observed with the use of an objective with a magnification factor of 250×. A Coherent Fieldmaster power meter placed on the sample holder was used for the determination of the laser power incident on the samples. The power reaching the sample decreased significantly with the objective magnification. For example, the incident power on the target is 3 and 0.5 mW when using the 100× and 250× objectives, respectively. Raman spectra reported here are not corrected for differences in incident power and instrument response or detector sensitivity.

* Corresponding author. E-mail: mcastro@uprm.edu.
† Visiting scholars. Permanent address: Transportation Security Administration, Federal Aviation Administration Technical Center, Atlantic City, NJ, 08405.

10.1021/jp0374206 CCC: $27.50
Published on Web 07/27/2004

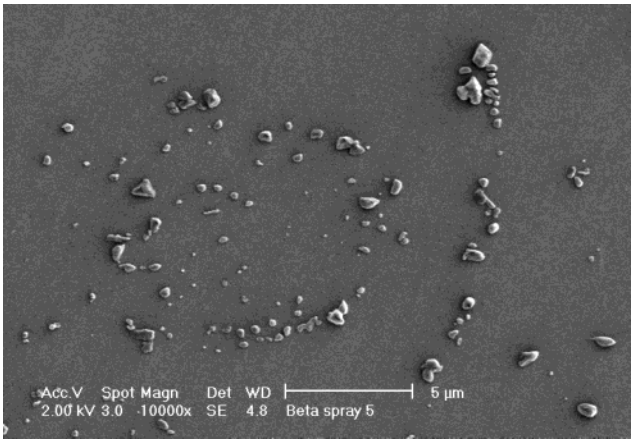

Figure 1. SEM image of glass substrate surface exposed to RDX in acetonitrile containing aerosol jet.

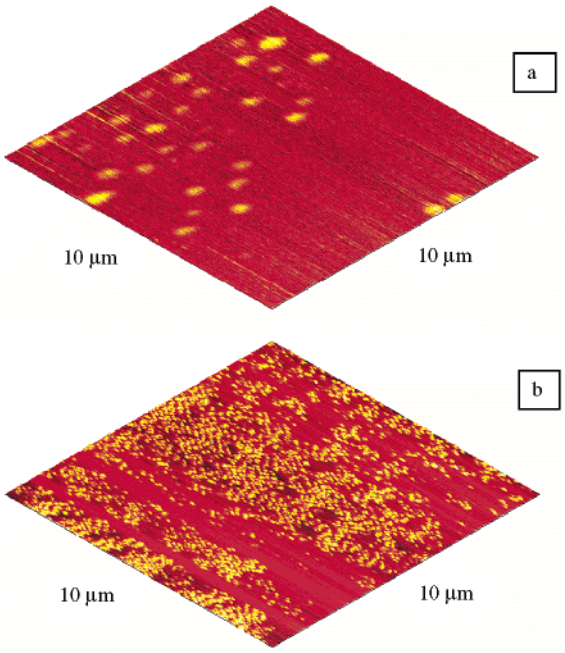

Figure 2. AFM images of RDX particles dispersed on a glass substrate using a (a) room temperature and (b) warmed aerosol jet.

3. Results and Discussion

SEM images of glass substrates exposed to five shots of the RDX aerosol jet are displayed in Figure 1. About 130 particles are scattered in the image displayed in Figure 1. The average size of the particles scattered in the image is 405 nm. The largest and smallest particles observed in the SEM image have diameters slightly over 1 μm and 160 nm, respectively. EDX measurements (not shown) on these particles revealed the presence of a peak distinctive from the background due to nitrogen atoms, as expected for RDX. Peaks due to carbon and oxygen are also observed in the EDX spectra of glass substrates exposed and not exposed to the RDX jet, limiting their use to establish the chemical composition of the nanoparticles.

In Figure 2 10 $\times$ 10 μm AFM images of RDX particles dispersed on glass substrate surfaces are displayed. The AFM measurement displayed in Figure 2a was performed on a glass substrate exposed to about three shots of the aerosol jet, containing RDX and acetonitrile. Patches of the bare glass substrate can be identified in the image. The RDX particles are clearly distinguishable from the substrate background. About 30 particles are displayed in the AFM image displayed in Figure 2a. Most of the particles have an ellipsoidal shape with an average size of 750 $\times$ 650 nm, with an uncertainty of $\pm$110 nm; this average particle size is slightly larger than the one obtained in SEM measurements of RDX nanoparticles prepared under identical conditions. The largest particle observed in the AFM image displayed in Figure 2a is about 1.15 μm; larger particles are observed in other regions of the sample. The roughness features found in substrate surfaces not exposed to the aerosol are (30 $\pm$ 10) nm. The height of the RDX nanoparticles ranges from 110 to 400 nm, larger than the roughness features found in substrates not exposed to the aerosol. Thus the distinctive particles in the AFM images displayed in Figure 2a are related not to the substrate, but to the formation of RDX nanoparticles.

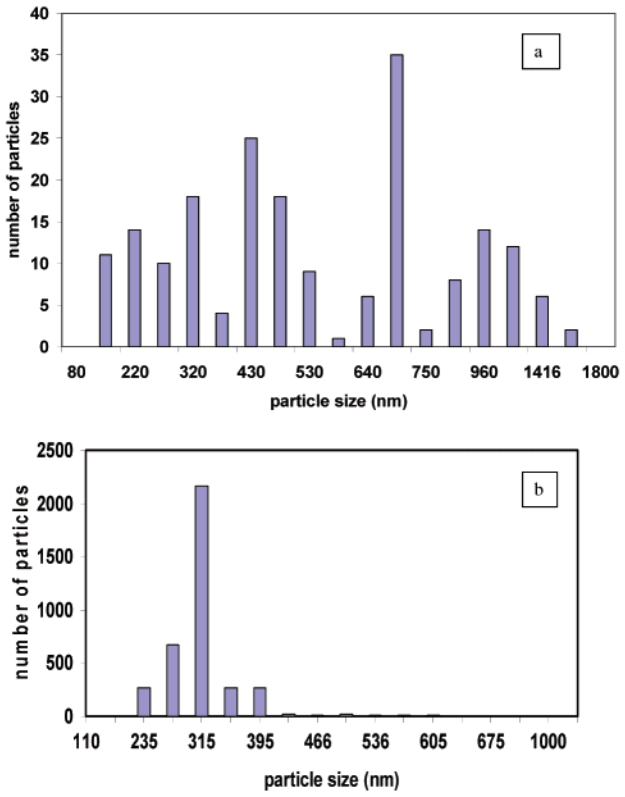

Figure 3. Particle size distribution obtained on different areas of substrates exposed to a (a) room temperature and (b) warmed aerosol jet.

Regions with a narrower particle size distribution can be found on the substrate when the solvent is evaporated from the RDX in acetonitrile jet in its flight to the target. A 10 $\times$ 10 μm AFM image of a region of a substrate exposed to an RDX aerosol jet warmed by a beam of N_2 gas during its flight to the target is displayed in Figure 2b. The particles are about (350 $\pm$ 60) nm in diameter and have a height of (360 $\pm$ 50) nm. The similarity in the diameter and height of the particles leads us to conclude that they have a nearly spherical shape.

Particle size distributions, obtained from analysis of SEM and AFM measurements, of substrates exposed to room temperature and warmed RDX aerosol jets are summarized in parts a and b, respectively, of Figure 3. Deposition of the particles with a room temperature aerosol results in the formation of particles with a diameter as high as 1.8 μm and an average particle size of 584 nm. RDX deposits prepared with a warmed aerosol result in the formation of particles with diameters between 160 and 780 nm and an average particle size of 380 nm. The elimination of a (solvent) medium that allows for the

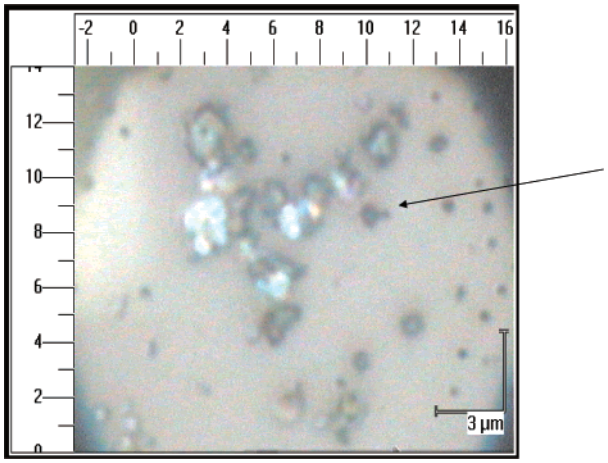

Figure 4. White light image of RDX nanoparticles dispersed on a glass substrate surface. The rulers are calibrated in micrometers. The internal scales indicated at the bottom right-hand corner of the image correspond to 3 μm. The arrow is used to guide the eye.

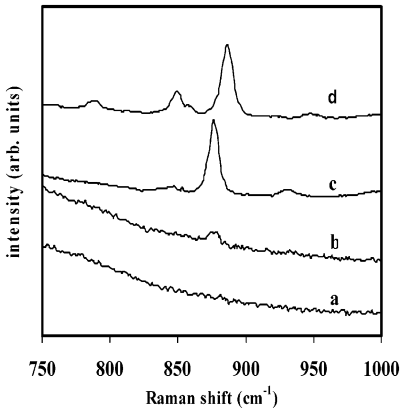

Figure 5. Raman spectra of (a) glass substrate, (b) RDX particle, (c) β RDX deposits, and (d) α RDX deposits, between 750 and 1000 cm^{-1}.

agglomeration of the particles results in the formation of RDX deposits with particles smaller than 1 μm.

A typical white light image of the RDX nanoparticles deposited with a room temperature aerosol on a glass substrate surface is displayed in Figure 4. The size of the particle indicated by the arrow is about 700 nm; smaller particles are scattered in the microscope field of view captured in Figure 4. Raman spectra between 750 and 1000 cm^{-1} of the RDX nanoparticles and samples of β and α RDX deposits on glass substrates are displayed in Figure 5. The spectrum of the glass substrate surface is also shown in Figure 5. The Raman spectrum of the glass substrate does not show any peaks between 750 and 1000 cm^{-1}. The Raman spectrum of the RDX particle was obtained by focusing the laser light through a 250× objective on the particle indicated by the arrow in Figure 4. The only peak observed in the Raman spectrum of the RDX particle is centered at 877 cm^{-1}. The band at 877 cm^{-1} is observed in Raman spectra obtained in other regions of the substrate where the particles are observed.

The spectroscopic signature of RDX has been used in this and other laboratories to distinguish between β and α RDX, the two known phases of this material. [4] Raman spectra of the β and α RDX deposits were measured with the purpose of establishing the chemical nature of the dispersed nanoparticles. A 500 ppm RDX in acetonitrile solution was employed for the preparation of the β and α RDX deposits. The β and α RDX deposits were prepared on the glass substrate surface in 0.5 and 12.0 μL quantities, respectively. The β and α RDX deposits used for the Raman measurements reported here have a diameter of 30 and 14 μm, respectively. The Raman spectra of β and α RDX were obtained with a 100× objective.

The band at 877 cm^{-1} has the highest intensity in the Raman spectrum of β RDX deposits. Peaks of smaller intensities at 847 and 933 cm^{-1} are clearly distinguishable above the baseline in the Raman spectrum of the β RDX deposit. This pattern of Raman peaks represents the spectroscopic signature of β RDX between 750 and 1000 cm^{-1}. Based on previous work, the band at 877 cm^{-1} is assigned to the ring-breathing mode in RDX.[3−4,12] Similar to the Raman spectra of cyclopentane and cyclohexane, the band due to the ring-breathing mode has the highest intensity between 800 and 900 cm^{-1}.[15]

The Raman spectrum of α RDX deposits, on the other hand, is dominated by the ring-breathing mode at 884 cm^{-1} and peaks of smaller intensity at 947, 861, 850, and 790 cm^{-1}. The spectroscopic signature of α RDX between 750 and 1000 cm^{-1} is consistent with previous Raman measurements on this phase.[4,5] The difference in the Raman spectra of β and α RDX has been attributed to the different structures of RDX in these forms of the material.[4,5] C_{3v} symmetry and C_s symmetry have been deduced for RDX molecules in the β and α forms, respectively. The larger number of peaks in the Raman spectrum of α RDX than in the Raman spectrum of β RDX has been attributed to the lower symmetry of molecules in the α phase than in the β form of the material.[4−5]

The ring breathing mode frequency is centered at 877 cm^{-1} in the Raman spectra of RDX nanoparticles and β deposits. This similarity leads us to propose that RDX molecules have similar chemical environments and molecular structure in the dispersed nanoparticles and in β RDX. The absence of the low-intensity signals at 847 and 933 cm^{-1} in the Raman spectrum of the dispersed nanoparticles is attributed to the reduced laser intensity that strikes the substrate in our experimental setup and the smaller amount of RDX examined. The smallest RDX nanoparticles characterized by vibrational spectroscopy in this work have a diameter of about 700 nm and have a spectroscopic signature consistent with β RDX. To our knowledge, these are the smallest particles of this material characterized with vibrational spectroscopy.

The physical chemistry of β RDX has eluded scientists for many years. Recent results obtained in this laboratory have established the presence of micrometer-sized particles in β RDX deposits. The results presented here are consistent with the observation of particles in β RDX deposits. The similarity in the spectroscopic properties of the dispersed nanoparticles and β RDX is, nevertheless, surprising. If particle−particle interactions play an important role in the spectroscopic properties of RDX, it is reasonable to expect differences between the Raman spectra of the dispersed nanoparticles and β RDX. The similarity in the ring breathing mode frequency among the nanoparticles and β RDX leads us to conclude that particle−particle interactions may not play an important role in the spectroscopic properties of β RDX.

Six conformers are predicted for gas-phase RDX.[5] The ring breathing mode frequency is predicted to have different values for the different gas-phase RDX isomers. The fact that the particles and β RDX have similar ring breathing mode frequencies leads us to conclude that only one isomer, the one with all NO_2 groups in axial position with respect to the triazine ring, is present in the nanoparticles examined here with vibrational spectroscopy. We cannot rule out the presence of other isomers in smaller RDX particles. Further experiments with near-field

optical microscopy are necessary to characterize smaller RDX nanoparticles.

4. Summary

In conclusion, we have used an aerosol jet containing RDX for the preparation of RDX nanoparticles, the smallest particles of this high-energy material reported in the literature. The RDX nanoparticles were characterized with AFM, SEM, white light imaging measurements, and Raman microscopy. The particle size distribution of the RDX nanoparticles depends on the deposition conditions. The smallest particles found in SEM measurements have a diameter of 160 nm. AFM measurements reveal particles with an elliptical shape in samples exposed to room temperature RDX in acetonitrile aerosol jet. These particles are about 750 × 650 nm in size. A narrower size distribution is observed in measurements performed on substrate surfaces exposed to an RDX aerosol jet warmed with hot nitrogen gas during its flight to the target. The diameter of these particles is about 350 nm. The spectroscopic signature of submicrometer RDX particles was also determined. RDX nanoparticles and β RDX deposits have a similar spectroscopic signature between 750 and 1000 cm^{-1}. The ring breathing mode frequency in RDX nanoparticles and β RDX deposits is centered at 877 cm^{-1}, about 7 cm^{-1} lower than α RDX.

Acknowledgment. Partial financial support for the operations of the CIC from the Federal Aviation Administration (FAA), Grant 99-G-029, and the Puerto Rico Infrastructure and Development Company (PRIDCO) and the National Science Foundation (Award No. 0304348) are gratefully acknowledged. Financial support from the Department of Defense (Contract No. DAAD 19-02-1-0257) for the operations of the CCSD is also acknowledged. We wish to acknowledge Aaron LaPointe from NVESD and Dr. Alberto Santana for proofreading the manuscript. We also thank Gabriel Cruz, from Hewlett-Packard in Aguadilla, Puerto Rico, for his assistance with the SEM measurements.

References and Notes

(1) Phares, D. J.; Holt, J. K.; Gregory, M. S.; Smedley, T.; Flagan, R. *J. Forensic Sci.* **2000**, *45*, 774−784.

(2) Akhavan, J. *The Chemistry of Explosives*; RSC Paperbacks: Athenaeum Press, Ltd.: Manchester, U.K., 1998.

(3) McCrone, W. C. *Anal. Chem.* **1950**, *22*, 954−953.

(4) Karpowicz, R. J.; Brill, T. B. *J. Phys. Chem.* **1984**, *88*, 348−352.

(5) Rice, B. M.; Chabalowski, C. F. *J. Phys. Chem. A* **1997**, *101*, 8720−8726.

(6) Choi, C. S.; Prince, E. *Acta Crystallogr., Sect. B* **1972**, *28*, 2857.

(7) Orloff, M. K.; Mullen, P. A.; Rauch, F. C. *J. Phys. Chem.* **1970**, *74*, 2189.

(8) Trinquecoste, C.; Rey-Lafon, M.; Forel, M. *J. Chem. Phys.* **1975**, *72*, 689.

(9) Rey-Lafon, M.; Trinquecoste, C.; Cavagnat, R.; Forel, M. *J. Phys. Chem.* **1970**, *68*, 1533−1542.

(10) Filhol, A.; Clement, C.; Forel, M.; Paviot, J.; Rey-Lafon, M.; Richoux, G.; Trinquecoste, C.; Cherville, J. *J. Phys. Chem.* **1971**, *75*, 2056.

(11) Cheng, C.; Kirkbride, T. E.; Batchelder, D. N.; Lacey, R. J.; Sheldon, T. G. *J. Forensic Sci.* **1995**, *40*, 31−37.

(12) Fell, N. F.; Vanderhoff, J. A.; Pesce-Rodriguez, R. A.; McNesby, K. L. *J. Raman Spectrosc.* **1998**, *29*, 165−172.

(13) Armstrong, R. W.; Baschung, B.; Booth, D. W.; Samirant, M. *Nano Lett.* **2003**, *3*, 253−255.

(14) Orloff, M. K.; Mullen, P. A.; Rauch, F. C. *J. Phys. Chem.* **1970**, *74*, 2189.

(15) Lin-Vien, D.; Colthup, N. B.; Fateley, W. G.; Grasselli, J. G. *The Handbook of Infrared and Raman Characteristic Frequencies of Organic Molecules*; Academic Press: San Diego, CA, 1991.